Thermal annealing effect on the nanomechanical properties and structure of P3HT: PCBM thin films

P.G. Karagiannidis, S. Kassavetis, C. Pitsalidis, S. Logothetidis *

Lab for Thin Films-Nanosystems and Nanometrology, Department of Physics, Aristotle University of Thessaloniki, GR-541 24 Thessaloniki, Greece

ARTICLE INFO

ABSTRACT

Nanostructured polymer–fullerene thin films are among the most prominent materials for application in high efficient polymer solar cells. Specifically, poly(3-hexylthiophene) (P3HT) and fullerene derivatives (PCBM) blends are used as the donor/acceptor materials forming a bulk heterojunction. Although P3HT:PCBM properties have been extensively studied, less light has been set on its nanomechanical properties, which affect the device service life. In this work Atomic Force Acoustic Microscopy (AFAM), Atomic Force Spectroscopy and Nanoindentation were used to study the effect of the fullerene presence and the annealing on the P3HT:PCBM nanomechanical behavior. The P3HT:PCBM thin films were prepared by spin coating on glass substrates and then annealed at 100 °C and 145 °C for 30 min. Large phase separation was identified by optical and Atomic Force Microscopy (AFM) for the annealed samples. Needle-like PCBM crystals were formed and an increase of the polymer crystallinity degree with the increase of the annealing temperature was confirmed by X-ray diffraction. AFAM characterization revealed the presence of aggregates close to stiff PCBM crystals, possibly consisting of amorphous P3HT material. AFM force–distance curves showed a continuous change in stiffness in the vicinity of the PCBM crystals, due to the PCBM depletion near its crystals, and the AFM indentation provided qualitative results about the changes in P3HT nanomechanical response after annealing.

© 2011 Elsevier B.V. All rights reserved.

1. Introduction

The development of organic photovoltaic (OPV) cells consisting of a polymer–fullerene bulk heterojunction (BHJ) has been rapid the last few years, due to their high technological interest. OPVs, which are close to commercialization, constitute an attractive low-cost renewable energy source. Especially, flexible solar cells deposited onto flexible polymeric substrates via large scale and roll-to-roll processes, present an attractive new low cost green technology [1–3]. Up to date, the polymer poly (3-hexylthiophene) (P3HT) blended with the fullerene derivative phenyl-C61-butyric acid methyl ester (PCBM), has been the most studied and successful system [4,5].

One of the most important factors for high efficiency OPVs, is the fabrication of the appropriate morphology of this active blend [5–8]. Ideally, the polymer and the fullerenes must be phase separated at 10–20 nm scale (typical exciton diffusion length) [8], providing thus large interfacial area for exciton dissociation. After charge separation the two phases must form pathways to the corresponding electrodes for efficient charge extraction. Unfortunately, this ideal situation is difficult to be achieved in practice. For the optimization of morphology, different experimental methods have been proposed such as post thermal annealing [9–11], solvent annealing [12] or the use of additives [13,14] which can lead to rearrangement of the spin coated film by crystallization of both phases. However, upon annealing large phase separation with the formation of micrometer size PCBM crystals usually occurs. The growth mechanism of these crystals has been recently studied by several research groups [15–18] in order to understand better the diffusion and crystallization of fullerenes within the polymer matrix.

Scanning Probe Microscopy techniques, such as Conductive AFM (C-AFM), Kelvin Probe Microscopy (KPM) [19–22], as well as Scanning near field Optical Microscope (SNOM) [16,23], have been used to study BJHs and provide useful information about their morphology as well as the charge transport mechanisms.

In this work, we study the effect of post thermal annealing on the nanoscale mechanical properties of large phase separated P3HT:PCBM BHJs using Atomic Force Acoustic Microscopy (AFAM), Atomic Force Spectroscopy and Nanoindentation in correlation with their morphology and structure. Phase identification and characterization, as well as local elasticity, are addressed using different techniques and their suitability for the study of organic thin films, such as BHJs, is discussed.

2. Experimental

For this study, regioregular P3HT with an average molecular weight $M_n = 45{,}000–65{,}000$ and PCBM were purchased from Aldrich.

* Corresponding author.
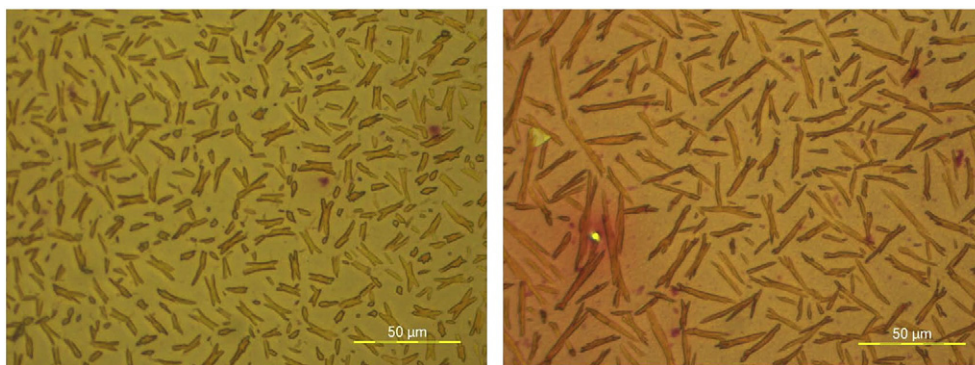*E-mail address:* logot@auth.gr (S. Logothetidis).

Fig. 1. Optical microscopy images of the P3HT:PCBM annealed: at 100 °C (left) and 145 °C (right) for 30 min.

A solution of the blend P3HT:PCBM (1:0.8 w/w) was prepared in chlorobenzene with a total concentration of 18 mg/ml. The solution was stirred at for least 24 h and filtered prior to spin coating through a 0.45 μm syringe filter. Samples were prepared by spin coating (1000 rpm for 30 s) on microscope glass slides under nitrogen atmosphere in a glove box. The glass substrates were carefully cleaned: first with a detergent and then they were ultrasonicated in deionized water, acetone, isopropanol and methanol. Finally, they were dried on a hot plate and then were UV irradiated for 10 min. After spin coating the annealing procedure was done on a hot plate inside a glove box. For simplicity the unannealed sample will be referred as Sample-RT and the annealed samples as Sample-100 (100 °C) and Sample-145 (145 °C).

For the Nanoindentation (NI) testing, the Continuous Stiffness Measurements option of the NanoIndenter XP was used, in order to study the nanomechanical properties of the P3HT:PCBM nanocomposites. The indents were made in several regions of the samples and specifically among the PCBM crystals in the case of the annealed samples, using a Berkovich diamond indenter. The hardness of the thin films is continuously measured versus the penetration depth using the following equation:

$$H = \frac{P}{A(h_c)} \qquad (1)$$

where P is the normal applied load and $A(h_c)$ is the contact area between the indenter and the sample. The h_c is the indentation contact depth estimated using the Oliver–Pharr method [24].

AFAM and Atomic Force Spectroscopy (AFS) measurements were made with a Scannning Probe Microscope (SOLVER P47 SPM, NT-MDT). AFAM measurements were performed in contact mode, using rectangular silicon cantilevers with 10 nm nominal tip curvature. More details about the cantilever geometrical characteristics used for AFS are given in the results and discussion section. AFAM was employed for the investigation of the near-surface mechanical properties of the P3HT:PCBM thin films. AFAM is a non destructive AFM technique, in which the AFM probe scans the sample's surface in contact mode and "records" the out-of-plane vibrations of the sample surface, which are caused by longitudinal acoustic waves emitted by a piezoelectric transducer, with 2.5 MHz central frequency. The transducer is placed below and in contact with the sample. This technique can provide sharp contrast variations of elasticity, while topography is simultaneously recorded in contact mode [25].

The X-ray study was performed with a D-5000 Siemens diffractometer, equipped with a conventional Cu Ka source. Information about the structural characteristics of the P3HT:PCBM thin films was deduced by employing the X-ray diffraction (XRD) technique. The XRD measurements were performed at the 3–30° angular range, where the main reflections of the P3HT and the PCBM are apparent, with 0.04° step size and 0.5°/min scan speed.

3. Results and discussion

The thermal annealing of the P3HT:PCBM nanocomposites at 100 °C and 145 °C for 30 min caused the formation of large PCBM crystals, as it is shown in the optical microscopy images (Fig. 1). In sample-RT, these needle-like features (the PCBM crystals) are not visible. The size of the needle-like PCBM crystals is up to 20 μm and 50 μm, for T = 100 °C and T = 145 °C respectively, with random orientation [15–18]. In addition, smaller disc-like crystals are present, which possibly correspond to an earlier stage of the needle-like crystal growth. In areas where the density of the crystals is high, brush-like needles and pinholes are also observed.

The structural analysis of the samples was made using X-ray diffraction (XRD). Fig. 2 illustrates the effect of annealing on the structure of the P3HT:PCBM thin films. All the XRD profiles show a peak at 5.20° to 5.24°, which is associated with the (100) reflection of the P3HT. Specifically, this peak corresponds to a-axis orientation, with the main polymer chain parallel and the side chains perpendicular to substrate [26]. After annealing, the intensity of this peak increases, indicating an improvement of the degree of crystallinity. In addition, intense peaks at 13.9° and 16.7°, as well as less intense ones at 25.3° and 29.3°, associated with the PCBM, are observed. The foregoing peaks are the result of PCBM diffusion in the polymer matrix and the formation of large PCBM crystals, as shown in Fig. 1 [27]. The size of the P3HT crystallites was calculated using the (100) reflection and the Scherrer formula:

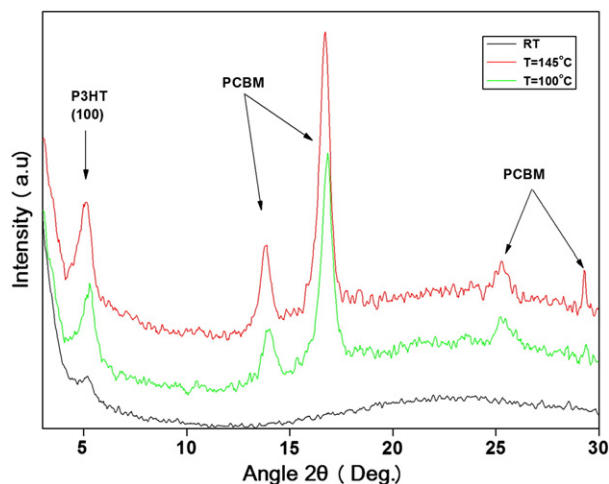$$D_{hkl} = 0.9\lambda \, / \, \beta_{hkl}\cos\theta \qquad (2)$$

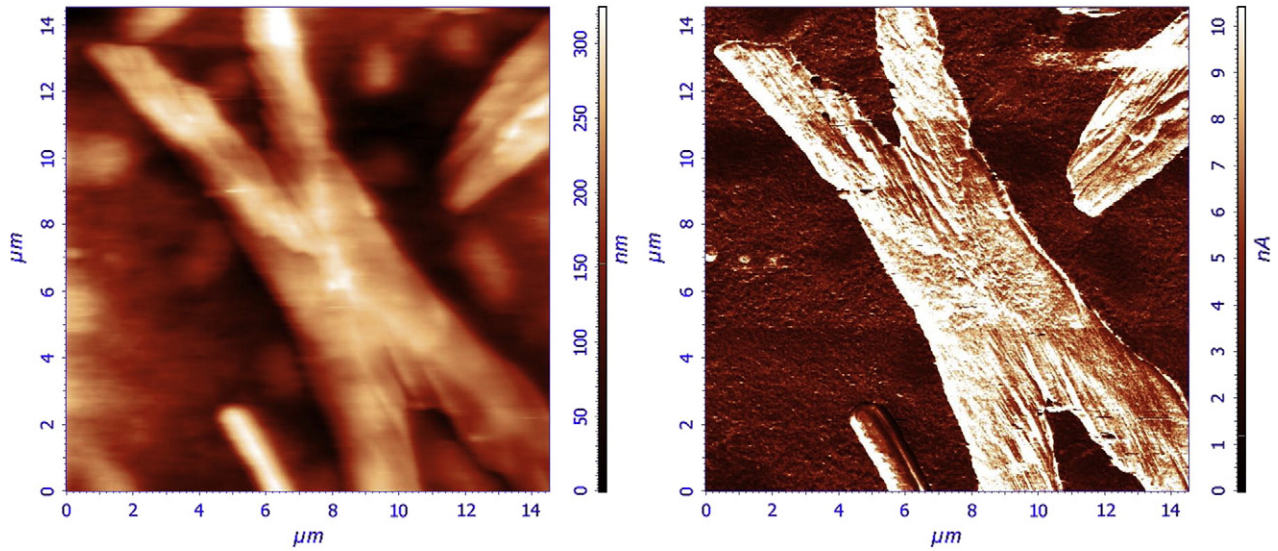Fig. 2. XRD patterns of the P3HT:PCBM thin films before (RT) and after annealing at 100 °C and 145 °C for 30 min.

Fig. 3. AFM topography (contact mode) and the corresponding AFAM image. Scan size is 14.5×14.5 μm^2.

where D_{hkl} is the apparent crystallite size along the [hkl] direction and β_{hkl} is the full width at half maximum (FWHM) of an (hkl) diffraction (in radians). Statistical analysis of the peak profile reveals an increase of the FWHM (D_{100}) (0.47° to 0.55°) with the increase of the annealing temperature and as consequence, a decrease of the P3HT grain size. Particularly, the P3HT crystallite size for sample-RT is 16.8 nm, whereas of the annealed samples at 100 °C and 145 °C is 15.5 nm and 14.1 nm, respectively. The observed decrease of the P3HT crystallite size is associated with the disordering of the polymer chains caused by the large PCBM clusters [28].

The effect of annealing on the local near-surface nanomechanical properties was studied using AFAM. By setting the SPM probe (cantilever) in contact with the sample surface, the so-called acoustic images can be acquired, which represent the vibration amplitude of the cantilever. The latter vibrates in contact with the sample surface at a fixed frequency, close to the resonance one. The acoustic images of each sample were acquired simultaneously with the topographic ones, in order to study in terms of surface morphology and nanomechanical properties exactly the same surface areas of the samples.

AFAM enables the mapping of the surface mechanical properties so that the surface regions with different mechanical responses can be distinguished. In Fig. 3 the topography and the corresponding AFAM image of the P3HT:PCBM thin film annealed at 100 °C are presented. A

typical PCBM needle-like crystal with 20 μm length and 300 nm height can be seen. Disc-like crystals are also observed in the upright corner of the image. In the topography image, the dark regions that surround the PCBM crystal indicate the large height deviation between the PCBM crystal and the polymer, which occurred by the PCBM molecules diffusion into the growing crystal and resulted to the local decrease of the thin film thickness [29]. In addition, P3HT aggregates are observed close to the PCBM crystals. In the AFAM image, the lighter surface regions correspond to material with greater stiffness. The PCBM crystals show sharp contrast comparing to the surrounding regions. While this was expected, the more interesting is that the P3HT aggregates, which are close to the PCBM crystals, appear to be darker compared to the rest of the P3HT. Thus, these aggregates are consisted of amorphous P3HT.

In Fig. 4 the NI hardness (H) of the P3HT:PCBM/glass samples, before (left) and after (right) annealing at 145 °C, versus the contact depth (h_c) is presented.

In the case of the sample-RT, the H values for $h_c = 0$–40 nm appear to be higher than those of the value plateau (H ≈ 0.25 GPa) for $h_c > 40$ nm. This happens due to: i) the NI inherent limitations. The A(h_c) does not accurately describe the indenter geometry for very swallow depths and as a consequence the H is overestimated and ii) the nanocomposite organic material mechanical properties, which are generally time-
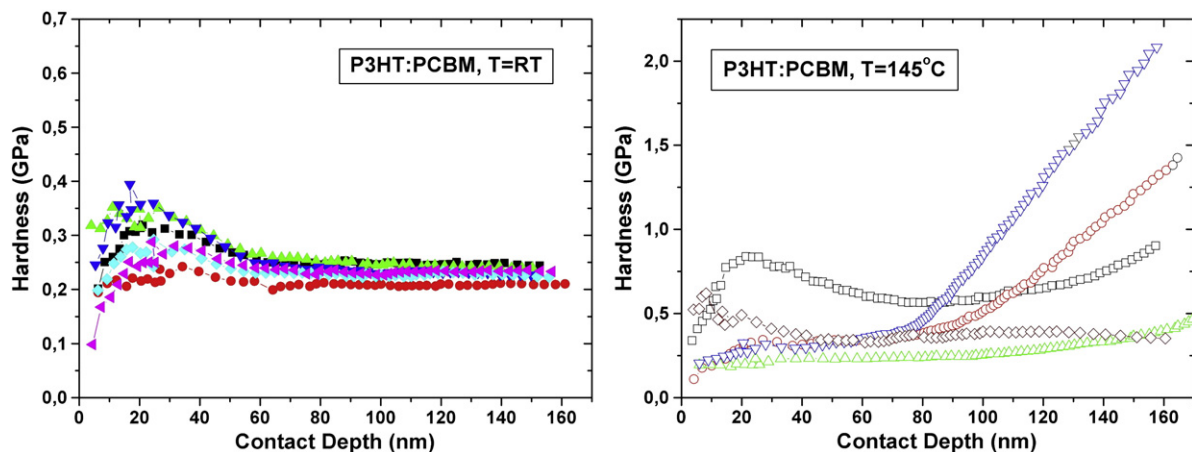

Fig. 4. The hardness of the P3HT:PCBM, before (left) and after the annealing at 145 °C (right), versus the nanoindentation contact depth.
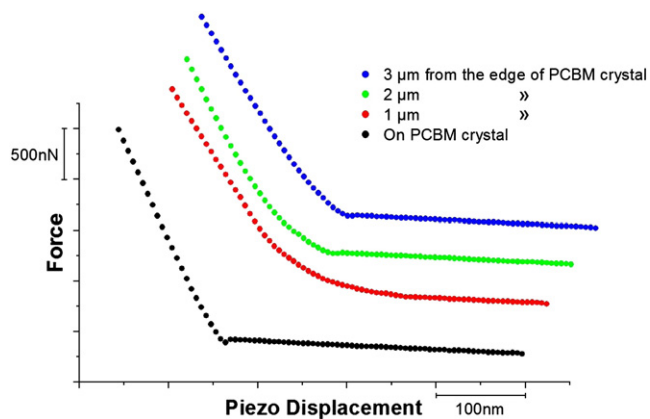
Fig. 5. Representative Force (nN)–Piezo Displacement (nm) curves on PCBM crystal and in various distances from the edge of the PCBM crystal.

depended. It should also be noted that the nanomechanical behavior of the sample-RT is uniform, because the H values at the plateau region are almost the same no matter the surface location of the indent.

In contrast, the H values of the annealed P3HT:PCBM coming from different indents present a variation that corresponds to an inhomogeneous material. The indents to this sample were made in regions between the PCBM crystals. Also, an abrupt increase of the H values after a certain h_c is observed. This happens due to the so-called substrate effect [30]. The substrate effect at the different surface locations starts at different h_c due to the inhomogeneous P3HT:PCBM thickness, which is occurred after the annealing.

Atomic Force Spectroscopy has been successfully used for the investigation of the local mechanical properties of soft, polymeric and biological materials [31]. Using cantilevers with low spring constant (k), forces in the range of nN can be applied and deform the sample. The elastic deformation of the samples is commonly evaluated with elastic continuum contact theories, such as the Hertzian and the Johnson–Kendall–Roberts [31].

In this work, stiff (k = 12–22.5 N/m), rectangular Si cantilevers and applied forces up to few μN were used to study the local mechanical properties of the P3HT:PCBM. It should be noted that: i) the cantilevers' tips are coated with 70 nm thick diamond coating and ii) the nominal radius of the tip curvature is 70 nm. The spring constant of each cantilever was measured by the normal Sader method [32], which is reliable for rectangular cantilevers.

Before AFS the samples were scanned in AFM semi-contact mode, in order to locate the appropriate surface regions. Then, for the AFS, switching to contact mode was made and a calibration of the optical system sensitivity was performed. The vertical deflection DFL (nA)

signal was recorded and converted to force by taking into account the cantilever's k and the Hooke's law. So, the corresponding Force (nN)–Piezo Displacement (nm) (F–D) curves were produced for each AFS at various locations on the sample's surface.

Over 100 curves at various applied loads were obtained at different sample areas of interest. Fig. 5 shows representative force–distance curves for the annealed Sample-100. The F–D curves are from the PCBM crystal and from regions at various distances from the PCBM edge (1–3 μm). The maximum applied force is 2 μN. On the right part of the curve (parallel to X-axis), the probe is approaching the surface and interact with the material via long range repulsive force. When the probe is close to the surface, the attractive Van der Waals and capillary forces cause a jump-in to contact with the sample's surface. This 'snap in to contact' point is easily defined on hard surfaces, like this of the PCBM crystal. From this contact point, the tip starts to apply force on the surface and the curve slope can provide information about the nanomechanical properties of the sample. Thus, from the F–D curves the PCBM appears to be stiffer than the surrounding P3HT material, in accordance with the AFAM results. The F–D curves show a progressive increase of the surface stiffness with the increase of the distance from the PCBM crystal edge. This means that the areas close to the PCBM crystals are P3HT-rich or PCBM-depleted [16,18].

Concerning the required force, which should be applied in order to plastically deform the several areas of the annealed P3HT:PCBM samples, it was found that:

i) For F ≤ 1 μN only the P3HT aggregates, which are close to the PCBM crystals, were plastically deformed.
ii) For F ≥ 4 μN (Fig. 6) the sample-RT was plastically deformed. For F = 4 μN, the indent impression was ~30 nm deep.
iii) For F ≈ 18 μN the annealed Sample-100 was plastically deformed and the indent impression was 28 nm deep.
iv) The maximum force that can be applied by this type of Si cantilevers is $F_{max} \approx 18$ μN and it was not possible to plastically deform the PCBM crystals with such low applied force.

In Fig. 6, the previously described residual impressions of the indents are presented.

4. Conclusions

Polyalkylthiophene/fullerene nanocomposites are the most promising materials for application in organic photovoltaic devices. Their efficiency is directly connected to the structure and phase separation, while the nanocomposite mechanical properties affect the device service life.

The effect of the thermal annealing on the structure and the surface distribution of the several structural features formed after annealing was studied in the light of their nanomechanical response. The increase of the thermal annealing temperature caused an increase to the size of
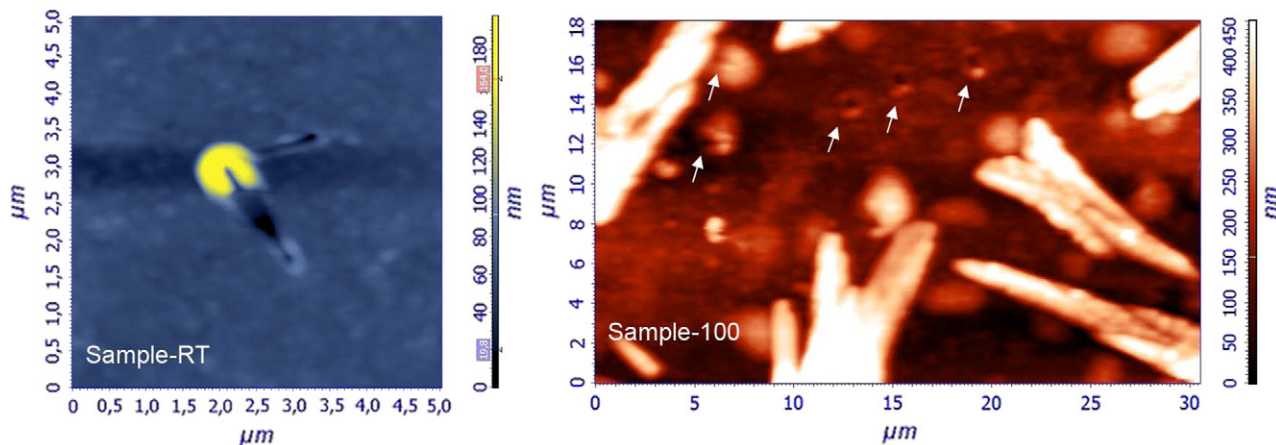

Fig. 6. AFM images showing the residual impression of the indents made on the surface of the P3HT:PCBM samples by AFS.

the PCBM crystallites and to the crystallinity of the two phases (PCBM and P3HT). In addition to the capability of measuring with nanometer precision the local mechanical properties of BHJs by AFM Force Spectroscopy, in both elastic and plastic regimes, enabled the discrimination of the several structural features of the P3HT and their mapping/distribution in relation to their distance from the PCBM crystallites.

Acknowledgements

References

[1] S. Logothetidis, Mater. Sci. Eng., B 152 (2008) 96.
[2] A.C. Mayer, S.R. Scully, B.E. Hardin, M.W. Rowell, M.D. McGehee, Mater. Today 10 (2007) 28.
[3] M.-C. Choi, Y. Kim, C.-S. Ha, Prog. Polym. Sci. 33 (2008) 581.
[4] P.A. Troshin, H. Hoppe, J. Renz, M. Egginger, J.Yu. Mayorova, A.E. Goryachev, A.S. Peregudov, R.N. Lyubovskaya, G. Gobsch, N.S. Sariciftci, V.F. Razumov, Adv. Funct. Mater. 19 (2009) 779.
[5] H. Hoppe, N.S. Sariciftci, J. Mater. Chem. 16 (2006) 45.
[6] S.S. van Bavel, E. Sourty, G. de With, J. Loos, Nano Lett. 9 (2009) 507.
[7] K. Maturova, S.S. van Bavel, M.M. Wienk, R.A.J. Janssen, M. Kemerink, Nano Lett. 9 (2009) 3032.
[8] P.A. Troshin, E.A. Khakina, M. Egginger, A.E. Goryachev, S.I. Troyanov, A. Fuchsbauer, A.S. Peregudov, R.N. Lyubovskaya, V.F. Razumov, N.S. Sariciftci, ChemSusChem 3 (2010) 356.
[9] Wanli Ma, Cuiying Yang, Alan J. Heeger, Adv. Mater. 19 (2007) 1387.
[10] F. Padinger, R.S. Rittberger, N.S. Sariciftci, Adv. Funct. Mater. 13 (2003) 85.
[11] W. Ma, C. Yang, X. Gong, K. Lee, A.J. Heeger, Adv. Funct. Mater. 15 (2005) 1617.
[12] G. Li, Y. Yao, H. Yang, V. Shrotriya, G. Yang, Y. Yang, Adv. Funct. Mater. 17 (2007) 1636.
[13] J.K. Lee, Wan L. Ma, C.J. Brabec, J. Yuen, J.S. Moon, J.Y. Kim, K. Lee, G.C. Bazan, A.J. Heeger, J. Am. Chem. Soc. 130 (2008) 3619.
[14] L.-M. Chen, Z. Hong, G. Li, Y. Yang, Adv. Mater. 21 (2009) 1434.
[15] A. Swinnen, I. Haeldermans, M. vande Ven, J. D'Haen, G. Vanhoyland, S. Aresu, M. D'Olieslaeger, J. Manca, Adv. Funct. Mater. 16 (2006) 760.
[16] E. Klimov, W. Li, X. Yang, G.G. Hoffmann, J. Loos, Macromolecules 39 (2006) 4493.
[17] J. Jo, S.-S. Kim, S.-I. Na, B.-K. Yu, D.-Y. Kim, Adv. Funct. Mater. 19 (2009) 866.
[18] B. Watts, W.J. Belcher, L. Thomsen, H. Ade, P.C. Dastoor, Macromolecules 42 (2009) 8392.
[19] L.S.C. Pingree, O.G. Reid, D.S. Ginger, Adv. Mater. 21 (2009) 19.
[20] O. Douhéret, L. Lutsen, A. Swinnen, M. Breselge, K. Vandewal, L. Goris, J. Manca, Appl. Phys. Lett. 89 (2006) 032107.
[21] Y.-C. Huang, S.-Y. Chuang, M.-C. Wu, H.-L. Chen, C.-W. Chen, W.-F. Su, J. Appl. Phys. 106 (2009) 034506.
[22] H. Hoppe, T. Glatzel, M. Niggemann, A. Hinsch, M.Ch. Lux-Steiner, N.S. Sariciftci, Nano Lett. 5 (2) (2005) 269.
[23] M.-C. Wu, H.-H. Lo, H.-C. Liao, S. Chen, Y.-Y. Lin, W.-C. Yen, T.-W. Zeng, Y.-F. Chen, C.-W. Chen, W.-F. Su, Sol. Energy Mater. Sol. Cells 93 (2009) 869.
[24] W.C. Oliver, G.M. Pharr, J. Mater. Res. 7 (1992) 1564.
[25] NT-MDT, Atomic Force Acoustic Microscopy – Instruction Manual.
[26] T. Erb, S. Raleva, U. Zhokhavets, G. Gobsch, B. Stühn, M. Spode, O. Ambacher, Thin Solid Films 450 (2004) 97.
[27] D. Chirvase, J. Parisi, J.C. Hummelen, V. Dyakonov, Nanotechnology 15 (2004) 1317.
[28] M.-Y. Chiu, U.-S. Jeng, C.-H. Su, K.S. Liang, K.H. Wei, Adv. Mater. 20 (2008) 2573.
[29] H. Zhong, X. Yang, B. de With, J. Loos, Macromolecules 39 (2006) 218.
[30] S. Logothetidis, S. Kassavetis, C. Charitidis, Y. Panayiotatos, A. Laskarakis, Carbon 42 (2004) 1133.
[31] B. Cappella, G. Dietler, Surf. Sci. Rep. 34 (1999) 1.
[32] J.E. Sader, J.W.M. Chon, Rev. Sci. Instrum. 70 (10) (1999) 3967.